

CYCLIC BEHAVIOR OF REINFORCED CONCRETE HAUNCHED BEAMS FAILING IN SHEAR

Hans I. Archundia-Aranda¹ and Arturo Tena-Colunga²

¹ Ph.D. Candidate, postgraduate program, Universidad Nacional Autónoma de México, Mexico City, México

² Professor, Universidad Autónoma Metropolitana, Mexico City, México
Email: archundia_aranda@yahoo.com.mx, atc@correo.azc.uam.mx

ABSTRACT:

This paper presents the research results about the testing of ten prototype reinforced concrete haunched beams subjected to cyclic loading. Beams were designed to present shear failure. Two groups of beams were tested: a) beams without shear reinforcement, and b) beams with minimum shear reinforcement. The cyclic testing allowed to fully validating a previous proposed equation to estimate the shear strength of reinforced concrete haunched beams. From the obtained results, it can be observed that haunched beams have a different shear behavior with respect to prismatic beams, having higher deformation and energy dissipation capacities, among other reasons, because nonprismatic beams exhibit an arching action along the haunched length as the main resisting mechanism, that favors smoother cracking patterns.

KEYWORDS: Haunched beams, nonprismatic elements, reinforced concrete beams, shear strength

1. INTRODUCTION

Reinforced concrete haunched beams (RCHBs) are often used in midrise buildings because offer some structural and nonstructural advantages over the prismatic elements, such as the lateral stiffness to self-weight ratio, and easing the placement of the different facilities inside the building (meaning an interstory height reduction). Nevertheless, in some countries, to consider RCHBs as structural solution may involve higher construction costs due to special formwork and qualified construction workers. In particular, haunched beams have been used in RC buildings in Mexico City from a long time ago. Despite this fact, reinforced concrete guidelines in Mexico (NTCC, 2004) and the USA (ACI-318, 2005) do not provide specific recommendations to insure a ductile behavior in nonprismatic elements.



Figure 1 Typical RCHBs in buildings recently constructed in Mexico City

Although the German code (DIN 1045-1, 2001) and some textbooks (Park and Paulay 1975, MacGregor 1997, Muttoni *et al.* 1997, Nielsen 1999) have some brief recommendations for the shear design of RCHBs, these guidelines do not include experimental data. The experimental evidence available is reduced to monotonic tests of prototypes failed in shear (Debaiky and El-Niema 1982, Stefanou 1983, El-Niema 1988, MacLeod and Houmsi 1994, Tena-Colunga *et al.* 2008).

In order to insure the desirable ductile behavior of RCHBs, according to the capacity-design rules, it is necessary first to understand how sudden failures under monotonic and cyclic loads occur, for example, the shear failure. Once this goal is achieved, it can be possible to study how to warrant a ductile flexural failure.

Therefore, in this paper the experimental results of ten RCHBs designed to develop shear failure and tested under cyclic loading are presented.

2. DESCRIPTION OF TEST SPECIMENS

The geometry of prototypes RCHBs was defined according to a survey conducted in existing buildings in Mexico City (Figures 1 and 2). The width (b) for all beams was 22 cm, the effective span (L) was 280 cm, and the shear span (a) was 108.3 cm. The haunched length (L_h) at both beam ends was one-third the effective span ($L_h=L/3\approx 93.3$ cm). Five different linear tapering geometries were obtained by keeping constant the overall depth at each beam end ($h_{max}=45$ cm) and reducing the overall depth at the central prismatic length to $h_{min}=45$ (prismatic control element), 40, 35, 30 and 25 cm. Therefore, haunched angles from the horizontal (α) were 0° , 3.07° , 6.12° , 9.13° and 12.10° respectively. Moreover, the geometry of all prototypes satisfied the requirement $L/h > 5$ to be considered as slender beams by the Mexican code ($L/h_{max} > 5$). In addition, with the purpose of not magnifying the characteristic arching mechanism observed experimentally and analytically in haunched beams (Debaiky and El-Niema 1982, El-Mezaini *et al.* 1991), all prototypes were checked against the well-known a/d limiting ratio between slender beams and short beams ($a/d_{max} > 2.5$). The top and bottom reinforcement cover was 4 cm. Prototypes were simply supported and tested with concentrated loads (V) that were applied 10 cm from the vertex formed by the intersection of tapered section with the prismatic section towards the centerline. Loads and reactions acted through $2.54 \times 10 \times 22$ cm steel plates to avoid local bearing crushing failures. The load was measured with load cells at each point of load.

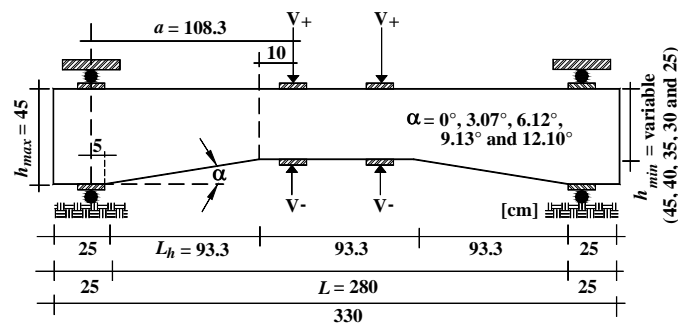


Figure 2 Geometry and loading condition for the test specimens

Table 1 Specifications of test specimens

Beam ID	α	Flexural reinforcement		Haunched length plus stub	Shear reinforcement	
		Top	Bottom		Prismatic length	Vertex
TASC α 0-R0-c	0°	3#8	4#8	1S#2.5	2S#2.5	-
TASC α 1-R0-c	3.07°	3#8	4#8	1S#2.5	2S#2.5	-
TASC α 2-R0-c	6.12°	3#8	4#8	1S#2.5	2S#2.5	-
TASC α 3-R0-c	9.13°	3#8	4#8	1S#2.5	2S#2.5	-
TASC α 4-R0-c	12.10°	3#8	4#8	1S#2.5	2S#2.5	-
TASC α 0-R1-c	0°	3#8	4#8	7S#2.5 @ 18.5 cm	2S#2.5 @ 18.5 cm	1S#2.5
TASC α 1-R1-c	3.07°	3#8	4#8	7S#2.5 @ 18.5 cm	2S#2.5 @ 18.5 cm	1S#2.5
TASC α 2-R1-c	6.12°	3#8	4#8	7S#2.5 @ 18.5 cm	2S#2.5 @ 18.5 cm	3S#2.5 @ 14.5 cm
TASC α 3-R1-c	9.13°	3#8	4#8	7S#2.5 @ 18.5 cm	2S#2.5 @ 18.5 cm	3S#2.5 @ 7.5 cm
TASC α 4-R1-c	12.10°	3#8	4#8	7S#2.5 @ 18.5 cm	2S#2.5 @ 18.5 cm	3S#2.5 @ 4.5 cm

Note: #8 bars = one inch diameter, # 2.5 bars = 5/16 inch diameter; S= stirrup

Two beams were constructed for each one of the five different geometries considered: a) one beam without shear reinforcement, only with four stirrups outside the shear span to hold the longitudinal steel reinforcement, and b) one beam with minimum shear reinforcement according to NTCC-04 for prismatic elements considering the effective depth at the support (d_{max}). Therefore, ten prototype haunched beams were tested. To insure a shear

failure along the haunches, the design was made providing the flexural capacity in the central prismatic length and keeping continuous the longitudinal reinforcement along the prototypes. The shear capacity at the haunched sections was checked with a semi-empirical equation proposed by Tena-Colunga *et al.* (2008). In addition, additional shear reinforcement was placed in the vertex of the prototypes with shear reinforcement. The specified material properties for design were a compressive strength $f'_c=250 \text{ kg/cm}^2$ for the concrete, and a yield tensile stress $f_y=4200 \text{ kg/cm}^2$ for all the steel reinforcement. The cryptogram for the identification of the prototypes is $TASC\alpha i-Rj-c$, where i is an index that indicates the considered haunched angle: $i=0=0^\circ$, $i=1=3.07^\circ$, $i=2=6.12^\circ$, $i=3=9.13^\circ$, and $i=4=12.10^\circ$; j is an index that indicates the shear reinforced: $j=0$ indicates the absence of shear reinforced whereas $j=1$ indicates the use of a minimum shear reinforced with the characteristic already referred. The reinforcement for each prototype is summarized in Table 1 and typical arrangements are shown in Figures 3 to 5.

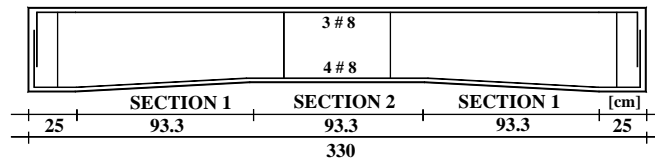


Figure 3 Reinforcement arrangement for beam TASCα1-R0-c

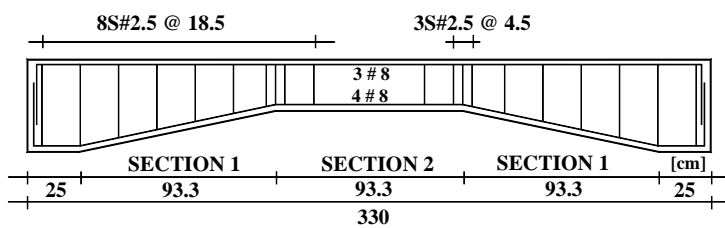


Figure 4 Reinforcement arrangement for beam TASCα4-R1-c

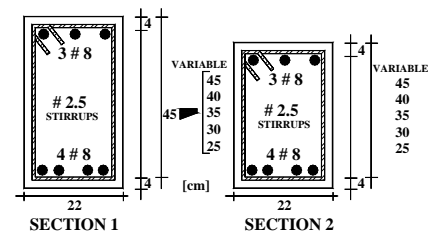


Figure 5 Typical cross sections

Each group of prototypes (with and without shear reinforcement) was tested according to a single deflection history where δ corresponds to the measured deflection at the midspan of the prototypes (Figure 6a). Positive loads (gravity direction) induce a positive moment and vice versa. The peak deflection increments in beams without shear reinforcement were 3 mm, whereas in beams with stirrups were 4 mm. For each complete cycle there was a complete cycle repetition. Tests were stopped when the beams lost the ability of support loads due to excessive damage (structural instability).

3. EXPERIMENTAL RESULTS

3.1. Hysteretic Response, Envelopes and Damage

The hysteretic response of prototypes with shear reinforcement is shown in Figure 7. The deflection (δ) at midspan was corrected by a fixed co-linear measurement to take into account the flexibility of the load testing device (Figure 6b). The shear force (V) corresponds to the haunched end where the failure occurred. Because of space constraints, the response of beams without shear reinforcement is not shown. A detailed discussion of experimental behavior in elements without shear reinforcement is presented in Tena-Colunga *et al.* 2007.

Because prototypes were subjected to the same deflection history, which means that deflection history is not a variable (Hwang y Scribner 1984), it is feasible to describe a general behavior for the RCHBs: increasing the haunched angle diminishes the shear capacity and the stiffness of the beams, but increases the number of cycles that can sustain and their deformation capacity. All elements exhibited a pinching at the origin which is characteristic of elements failing in shear (Brown and Jirsa 1971). In addition, it is evident a slight asymmetry in

the hysteresis due to: 1) the geometry and reinforcement asymmetry of the prototypes with respect to a longitudinal axis and, 2) their self weight.

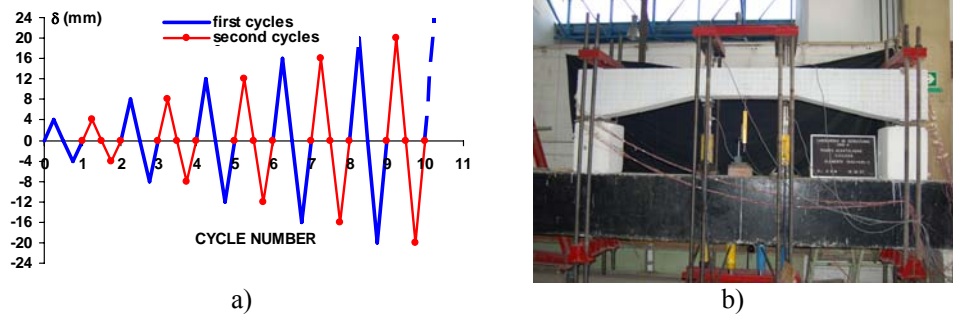


Figure 6 Experimental program: a) deflection history, and b) testing device (prototype TASC α 4-R1-c)

On the basis of experimental observations, three characteristic forces were identified from the full hysteretic response: 1) the shear force that caused the first diagonal cracking (V_{cr}), 2) the ultimate (maximum) shear force (V_u) and, 3) the shear that caused the collapse of the beams ($V_{collapse}$). All characteristic stages occurred under positive loads (Figure 2).

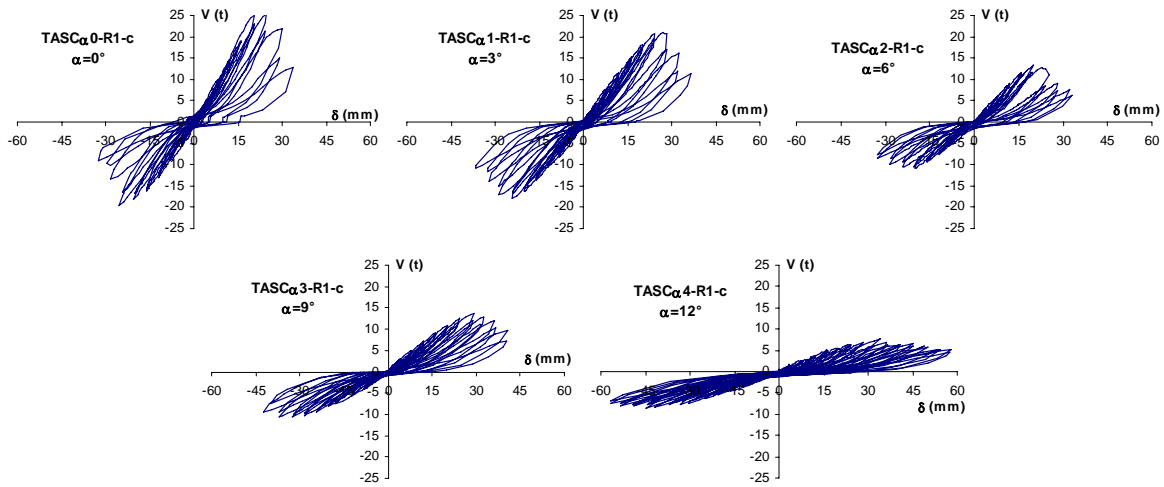


Figure 7 Hysteretic response of RCHBs with shear reinforcement

Table 2 Characteristic shear forces

Beam ID	f'_c (kg/cm ²)	V_{cr} (ton)	V_u (ton)	$V_{collapse}$ (ton)	V_{HB} (ton)
TASC α 0-R0-c	454	8.78	12.61	12.06	9.94
TASC α 1-R0-c	433	4.41	4.41	4.41	8.58
TASC α 2-R0-c	354	5.97	6.08	4.21	6.69
TASC α 3-R0-c	395	3.83	3.85	4.37	5.98
TASC α 4-R0-c	361	1.61	2.76	3.41	4.67
TASC α 0-R1-c	227	4.56	24.89	12.92	17.88
TASC α 1-R1-c	245	8.18	20.75	11.38	16.05
TASC α 2-R1-c	217	6.16	13.23	7.55	13.73
TASC α 3-R1-c	284	2.92	13.70	9.77	12.43
TASC α 4-R1-c	245	1.52	7.88	5.12	9.94

The characteristic shear forces already described are summarized in Table 2. Additionally, in the same Table 2 shear capacity predictions (V_{HB}) according to the equation proposed by Tena-Colunga *et al.* (2008) are also reported. The shear capacities were computed considering the measured properties for the concrete and steel

reinforcement. The measured compressive strength for the concrete is reported in Table 2. The measured yield stresses were $f_y=4348 \text{ kg/cm}^2$ for the longitudinal reinforcement and $f_y=4592 \text{ kg/cm}^2$ for the shear reinforcement. Finally, the displacements associated to each characteristic stage are summarized in Table 3.

Table 3 Characteristic displacements

Beam ID	δ_{cr} (mm)	δ_u (mm)	$\delta_{collapse}$ (mm)	Beam ID	δ_{cr} (mm)	δ_u (mm)	$\delta_{collapse}$ (mm)
TASC α 0-R0-c	6.06	12.10	18.10	TASC α 0-R1-c	4.14	20.42	33.60
TASC α 1-R0-c	6.12	9.48	19.00	TASC α 1-R1-c	8.04	24.10	36.46
TASC α 2-R0-c	6.14	8.88	24.30	TASC α 2-R1-c	8.00	20.02	32.40
TASC α 3-R0-c	6.10	9.22	30.22	TASC α 3-R1-c	4.06	29.28	40.56
TASC α 4-R0-c	3.08	18.14	60.46	TASC α 4-R1-c	4.08	33.92	57.88

The response envelopes for the beams with shear reinforcement are shown in Figure 8 where there is a distinction between *first* and *second* cycles envelopes. Graphics are in different scale to improve visualization.

From the reported values in Table 2 it is evident that the expected shear capacity in beams without shear reinforcement (R0-c beams) was overestimated. This can be explained by the fact that the absence of stirrups favored a more pronounced concrete degradation that was increased by load reversals (Gosain *et al.* 1977).

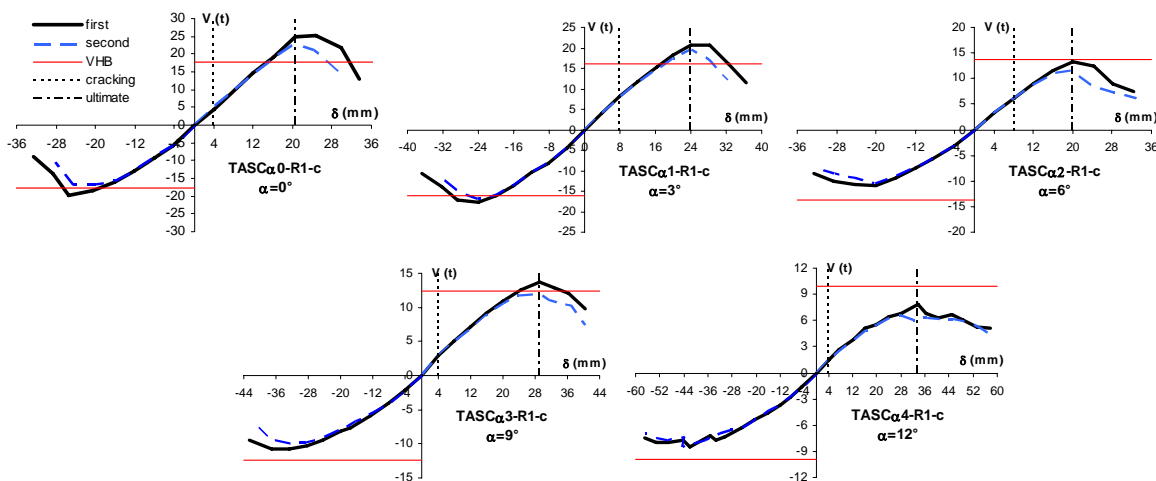


Figure 8 Envelopes for the RCHBs with shear reinforcement

As observed in monotonic testing, the shear capacity prediction was good principally in haunched beams up to haunched angles of nine degrees for the beams with minimum shear reinforcement. Beam TASC α 2-R1-c ($\alpha=6.12^\circ$) was tested at early age (32 days old) in comparison with the rest of the beams (200-250 days old). In addition, this element had the lower concrete strength. These facts favored an excessive flexural cracking along the element which could explain the adjusted strength observed.

Typical cracking patterns are shown in Figure 9. The cracking patterns at ultimate and collapse stages clearly show a full diagonal crack distribution along the shear span (haunched length). This crack pattern supports the well identified arching mechanism in monotonic test and analytical studies. The greatest deformation capacity observed in RCHBs in comparison with the prismatic elements is associated to the ability of RCHBs to redistribute the cracks. As a general rule, increasing the haunched angle increases the damage allowed and increases the pinching due to the sliding along the cracks. Moreover, the characteristic brittle and sudden shear failure of prismatic elements is reduced in RCHBs due to this behavior.

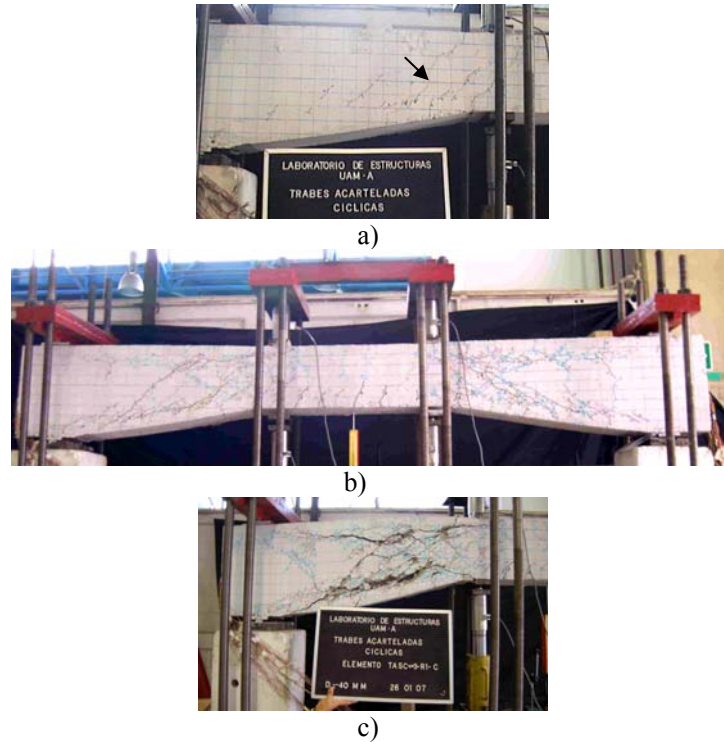


Figure 9 Cracking patterns in Beam TASC α 3-R1-c: a) first diagonal cracking, b) ultimate, and c) collapse

3.2. Stiffness Degradation

Peak to peak secant stiffness (K) was computed for each complete cycle and normalized with respect to the initial elastic stiffness (K_o). The elastic and normalized stiffnesses are summarized in Table 4 whereas the evolution of the stiffness degradation is depicted in Figure 10.

Table 4 Peak to peak stiffness

Beam ID	K_o (ton/mm)	K_{cr}/K_o	K_u/K_o	$K_{collapse}/K_o$	Beam ID	K_o (ton/mm)	K_{cr}/K_o	K_u/K_o	$K_{collapse}/K_o$
TASC α 0-R0-c	1.46	0.92	0.60	0.42	TASC α 0-R1-c	1.22	1.0	0.86	0.27
TASC α 1-R0-c	0.72	0.85	0.61	0.31	TASC α 1-R1-c	1.01	0.97	0.77	0.29
TASC α 2-R0-c	0.95	0.98	0.58	0.20	TASC α 2-R1-c	0.73	0.90	0.75	0.31
TASC α 3-R0-c	0.64	0.92	0.55	0.25	TASC α 3-R1-c	0.63	1.0	0.66	0.37
TASC α 4-R0-c	0.57	0.98	0.28	0.06	TASC α 4-R1-c	0.35	1.0	0.67	0.32

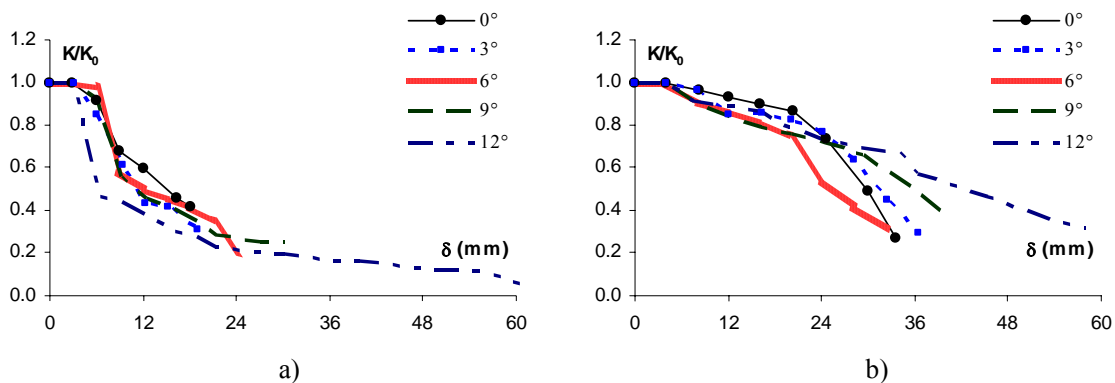


Figure 10 Peak to peak stiffness: a) beams without shear reinforcement and, b) beams with shear reinforcement

From the results reported in Table 4 and the graphics depicted in Figure 10 it is evident, and obvious, that the absence of stirrups increases the stiffness degradation rate. The Mexican code suggests that a cracked beam shall to remain a 50% of their initial stiffness properties at the moment to develop their flexure capacity. As can be observed from Table 4, RCHBs would be able to fulfill this requirement because even under a brittle failure (shear failure) the beams kept 60% of their original stiffness at the ultimate stage.

3.3. Energy Dissipation

Even though the haunch diminishes the concrete volume respect to a prismatic element, the experimental evidence shown that at least, RCHBs dissipate as much energy as prismatic beams (Table 5). Although the experimental results are clear about this fact, it is feasible to normalize the computed accumulated hysteretic energy at collapse (E_H) against the half-volume beam to point out the haunched effect (geometric effect). This concept is the *energy density* proposed by Popov (1998) and is depicted in Figure 11.

Table 5 Accumulated hysteretic energy

Beam ID	Half Volume (m ³)	Cracking		Ultimate		Collapse	
		E_H (ton x mm)	Cycle number	E_H (ton x mm)	Cycle number	E_H (ton x mm)	Cycle number
TASC α 0-R0-c	0.144	26.53	3	144.55	7	455.59	11.5
TASC α 1-R0-c *	0.133	8.99	3	36.78	5	189.15	11
TASC α 2-R0-c	0.123	8.66	3	55.37	5	413.88	15
TASC α 3-R0-c	0.113	4.94	3	30.69	5	564.20	20
TASC α 4-R0-c	0.102	0.39	1	116.21	11	2291.85	36.5
TASC α 0-R1-c	0.144	7.88	1	338.87	9	1345.47	15
TASC α 1-R1-c	0.133	33.74	3	499.63	11	1612.12	17
TASC α 2-R1-c *	0.123	20.64	3	198.94	9	904.19	16
TASC α 3-R1-c	0.113	4.53	1	491.53	13	1418.89	20
TASC α 4-R1-c	0.102	2.34	1	425.13	15	1739.62	28

* This elements had a premature failure

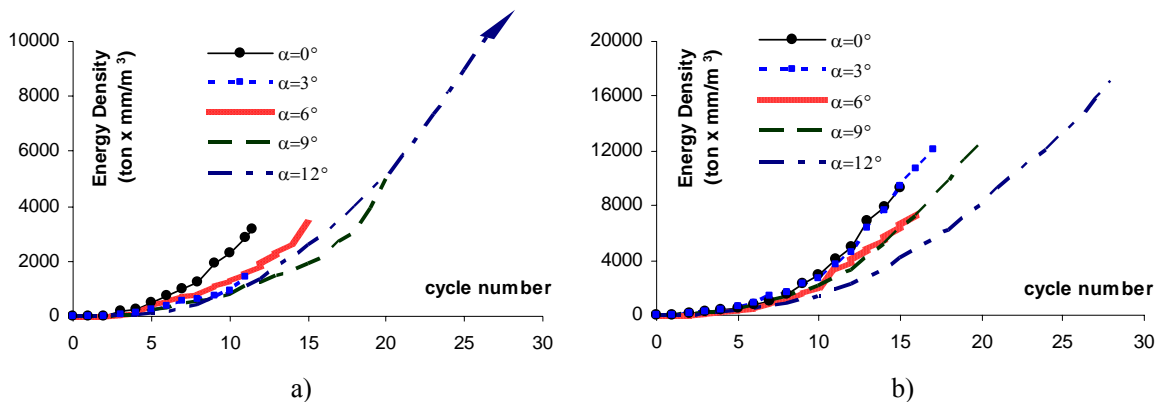


Figure 11 Energy density: a) beams without shear reinforcement, and b) beams with shear reinforcement

4. CONCLUDING REMARKS

This paper has presented some of the experimental results of the testing of ten reinforced concrete haunched beams (RCHBs) with and without shear reinforced designed to fail in shear under cyclic loading. It was observed that haunched beams develop an arch mechanism that improves the global shear behavior in comparison with the well-known shear behavior of prismatic elements. Haunched beams develop higher deformation and energy dissipation capacities and smoother cracking patterns than prismatic beams. Until more evidence would be available, it is advisable to estimate the shear strength of RCHBs with the equation proposed by Tena-Colunga *et al.* (2008) for beams up to nine degrees of haunched.

5. ACKNOWLEDGEMENTS

Financial support of Secretaría General de Obras del Gobierno del Distrito Federal and Universidad Autónoma Metropolitana are gratefully acknowledged. Appreciation is extended to Alejandro Grande and Leopoldo Quiroz for their invaluable participation in the construction and cyclic testing of these beams.

REFERENCES

- ACI-318-05. (2005). Building Code Requirements for Structural Concrete. *American Concrete Institute*.
- Brown R. H. and Jirsa J. O. (1971). Reinforced concrete beams under load reversals. *ACI Journal* **68:5**, 380-390.
- Debaiky S. Y. and El-Niema E. I. (1982). Behavior and strength of reinforced concrete haunched beams in shear. *ACI Journal* **79:3**, 184-194.
- DIN 1045-1. (2001). Concrete, Reinforcement and Prestressed Concrete Structures, Part 1: Design. *Deutsches Institut für Normung e.V.*
- El-Mezaini N., Balcaya C. and Citipitioglu E. (2001). Analysis of frames with nonprismatic members. *ASCE Journal of Structural Engineering* **117:6**, 1573-1592.
- El-Niema E. I. (1988). Investigation of concrete haunched T-beams under shear. *ASCE Journal of Structural Engineering* **114:4**, 917-930.
- Gosain N. K., Brown R. H. and Jirsa J. O. (1977). Shear requirements for load reversals on RC members. *ASCE Journal of Structural Engineering* **103:7**, 1461-1476.
- Hwang T. and Scribner C. F. (1984). R/C members cyclic response during various loadings. *ASCE Journal of Structural Engineering* **110:3**, 477-489.
- NTCC-2004. (2004). Normas Técnicas Complementarias para Diseño y Construcción de Estructuras de Concreto. *Gaceta Oficial del Gobierno del Distrito Federal*, octubre. (in Spanish).
- MacLeod I. A. and Houmsi A. (1994). Shear strength of haunched beams without shear reinforcement. *ACI Structural Journal* **91:4**, 79-89.
- MacGregor J. G. and Wight J. K. (2005). *Reinforced concrete-mechanics and design*, fourth edition, Pearson-Prentice Hall, USA.
- Muttoni A., Shwartz J. and Thürlimann B. (1997). *Design of concrete structures with stress fields*, Birkhäuser, Germany.
- Nielsen M. P. (1999). *Limit analysis and concrete plasticity*, second edition, CRC Press, USA.
- Park R. and Paulay T. (1975). *Reinforced concrete structures*, John Wiley and Sons, USA.
- Popov E. P. (1998). *Engineering mechanics of solids*, second edition, Prentice Hall, USA.
- Stefanou G. D. (1983). Shear resistance of reinforced concrete beams with non-prismatic sections. *Engineering Fracture Mechanics* **18:3**, 643-667.
- Tena-Colunga A., Archundia-Aranda H. I. and González-Cuevas O. M. (2008). Behavior of reinforced concrete haunched beams subjected to static shear loading. *Engineering Structures* **30:2**, 478-492.
- Tena-Colunga A., Archundia-Aranda H. I., Grande-Vega A and González-Cuevas O. M. (2007). Cyclic shear behavior of reinforced concrete haunched beams. *Ninth Canadian Conference on Earthquake Engineering, Ottawa-Ontario*.